



High ENSO sensitivity in tree rings from a northern population of *Polylepis tarapacana* in the Peruvian Andes



Doris B. Crispín-DelaCruz ^{a,*}, Mariano.S. Morales ^{a,b}, Laia. Andreu-Hayles ^{c,d,e}, Duncan. A. Christie ^{f,g}, Anthony Guerra ^h, Edilson. J. Requena-Rojas ^a

^a Laboratorio de Dendrocronología, Universidad Continental, Huancayo, Peru

^b Instituto Argentino de Nivología, Glaciología y Ciencias Ambientales, CONICET, Mendoza, Argentina

^c Lamont-Doherty Earth Observatory of Columbia University, New York, NY, United States

^d CREAF, Bellaterra (Cerdanyola del Vallés), Barcelona, Spain

^e ICREA, Pg. Lluís Companys 23, Barcelona, Spain

^f Laboratorio de Dendrocronología y Cambio Global, Instituto de Conservación Biodiversidad y Territorio, Universidad Austral de Chile, Valdivia, Chile

^g Center for Climate and Resilience Research (CR2), Chile

^h Missouri Botanical Garden, Prolong. Bolognesi Mz.E Lote 6, Pasco, Oxapampa, Peru

ARTICLE INFO

Keywords:

Tree-growth

Climate variability

Paleoclimate

Tropical dendroclimatology

Northwest Altiplano

Central Andes

ENSO proxy record

ABSTRACT

Polylepis tarapacana is the highest-elevation tree species worldwide growing between 4000 and 5000 m a.s.l. along the South American Altiplano. *P. tarapacana* is adapted to live in harsh conditions and has been widely used for drought and precipitation tree-ring based reconstructions. Here, we present a 400-year tree-ring width (TRW) chronology located in southern Peru (17°S; 69°W) at the northernmost limit of *P. tarapacana* tree species distribution. The objectives of this study are to assess tree growth sensitivity of a northern *P. tarapacana* population to (1) precipitation, temperature and El Niño Southern Oscillation (ENSO) variability; (2) to compare its growth variability and ENSO sensitivity with southern *P. tarapacana* forests. Our results showed that this TRW record is highly sensitive to the prior summer season (Nov-Jan) precipitation (i.e. positive correlation) when the South American Summer Monsoon (SASM) reaches its maximum intensity in this region. We also found a positive relationship with current year temperature that suggests that radial growth may be enhanced by warm, less cloudy, conditions during the year of formation. A strong positive relationship was found between el Niño 3.4 and tree growth variability during the current growing season, but negative during the previous growth period. Growth variability in our northern study site was in agreement with other populations that represent almost the full range of *P. tarapacana* latitudinal distribution (~ 18°S to 23°S). Towards the south of the *P. tarapacana* TRW network there was a decrease in the strength of the agreement of growth variability with our site, with the exception of higher correlation with the two southeastern sites. Similarly, the TRW chronologies recorded higher sensitivity to ENSO influences in the north and southeastern locations, which are wetter, than the drier southwestern sites. These patterns hold for the entire period, as well as for periods of high and low ENSO activity. Overall, *P. tarapacana* tree growth at the north of its distribution is mostly influenced by prior year moisture availability and current year temperature that are linked to large-scale climate patterns such as the SASM and ENSO, respectively.

1. Introduction

The complex topography of the Andes plays an important role in regulating part of the large-scale atmospheric circulation over South America, shaping a range of well-differentiated climates types in both sides of the Cordillera (Garreaud, 1999). In the tropical Central Andes is

located the South American Altiplano, a high altitude semi-arid plateau over ~ 4000 m a.s.l. between the eastern and western Cordillera and spanning from 15°S to 24°S with an average width of 300 km (Garreaud and Aceituno, 2001). In the last decades, the Altiplano have experienced persistent warming and drying trends (Ramos-Calzado et al., 2008), which are estimated to continue over the near future (Neukom et al.,

* Corresponding author.

E-mail addresses: doriscrispin@hotmail.com, 48287032@continental.edu.pe (D.B. Crispín-DelaCruz).

2015). Water resources from this region are critical for human consumption, ecosystems, agriculture, mining, hydropower and other socio-economic activities not only for this vast territory, but also for the dry western lowlands. In particular in the Peruvian Altiplano, traditional small-scale agriculture and subsistence farming is highly sensitive to drought and floods at inter-annual scale (Vargas, 2009), and as a consequence these activities and the rural lifestyle are vulnerable to extreme weather conditions presenting a high climate risk (Sietz et al., 2012). For example, the extreme drought of 1982–83 produced a severe crop failure of potatoes and quinoa which represent the main agriculture production in the region. Moreover, the widespread famine during this extreme event produced profound social impacts among the Andean settlers, leading to cases of children being sold to wealthier families as a way to escape hunger in desperate homes (Cavledes, 1985). Likewise, extreme frosts events can also negatively affect traditional crops and have triggered a high mortality of the camelid livestock (alpacas and llamas) and sheep (Andrade, 2018). One of the main drivers of extreme climatic conditions at interannual scale in the Altiplano is the El Niño-Southern Oscillation (ENSO) phenomenon (Garreaud and Aceituno, 2001; Vuille, 1999). The lack of crop insurances for rural communities places the Peruvian Andes as a very vulnerable region in relation to food security associated with strong ENSO events (Gilles and Valdivia, 2009). Thus, there is an urgent need to achieve a better understanding of climate variability and its drivers in the Central tropical Andes in order to improve strategies for disaster risk management.

The study of climate variability over the Central tropical Andes associated to major circulation patterns such as the ENSO and the South American Summer Monsoon (SASM) has been a topic of great interest in the scientific community during last decades (e.g. Vera et al., 2006; Garreaud et al., 2009). However, our understanding of the full range of climate variability for decadal and longer time scales have been limited due to the scarcity of meteorological stations and to the short span of the records, rarely exceeding 50 years in this complex mountain region (Drenkhan et al., 2015). This precludes the assessment of trends, low-frequency variability and return time of extreme event occurrence such as severe droughts and floods. In this context, the development of new high-resolution precipitation and ENSO proxies from tree rings can be useful to provide a multi-centennial range of climate variability in the study region from interannual, decadal and even centennial time scales.

Polylepis tarapacana Phill. grows across the South American Altiplano (16°S to 23°S) over the slopes of volcanoes up to 5200 m.a.s.l. and it is the highest elevation tree species worldwide (Kessler and Schmidt-Lebuhn, 2006). This tree species is well adapted to the Altiplano extreme conditions such as low temperatures, water scarcity and high solar irradiation (García-Plazaola et al., 2015). Because the growth of *P. tarapacana* is highly sensitive to variations in water availability (Argollo et al., 2004; Rodriguez-Catón et al., 2021), during the last decades records based on its ring-width variations have been successfully used to reconstruct past hydroclimate variability in the Central and Southern Altiplano (18°–23°S; Morales et al., 2020, 2015, 2012). Most *P. tarapacana* chronologies are located south of 18°S and so far none has been developed in Peru a the northern Altiplano, where the conditions are wetter and there is a higher exposure to ENSO influence (Trenberth and Caron, 2000). Here, we generated the longest *P. tarapacana* tree-ring width (TRW) chronology in Peru to provide a new high-resolution centennial record for this region and to address the following specific objectives. The goals of this study are: (1) to expand the present *P. tarapacana* TRW network to its northern distribution limit into the Peruvian Andes; (2) to assess the tree growth sensitivity of this new TRW chronology to precipitation, temperature and the ENSO variability; and (3) to compare its growth variability and ENSO sensitivity with other *P. tarapacana* southern locations.

2. Materials and methods

2.1. Study area

The study was carried out in a *P. tarapacana* forest located near to Chiluyo Village at 4657 m a.s.l. at the northern part of the South American Altiplano in the department of Tacna in Peru (17°24S, 69°39W, Fig. 1a). Biogeographically, this site is located in the xerophytic Puna region that is a high Andean ecosystem rich in endemic elements dominated by grasslands associated with scrub and shrubs of Cactacea, Fabacea, Zylophylaceae and Asteraceae families, in addition to *Polylepis* forests (Josse et al., 2009).

At the Mazocruz weather station, which is the nearest from the Chiluyo TRW site (74 km northeast; 16° 44S, 69° 42W; 4006 m a.s.l, Fig. 1b), the mean annual temperature is 4.8 °C with minimum and maximum temperatures ranging from –6.5 to 16.1 °C, respectively. The temperature amplitude is 7.73 °C. The total annual rainfall is 523 mm which is more than the double than the annual precipitation recorded at the southwestern species distribution limit adjacent to the Atacama Desert (Morales et al., 2018). The 81% of the annual precipitation occurs during the austral summer months (Dec-Mar) showing a clear unimodal distribution. The driest and wettest months are June (2 mm) and January (139 mm), respectively.

2.2. Tree-ring sampling and chronology development

We collected 43 cross sections from one of the multiple stems of the living individuals and wedges of dead trees. Following standard dendrochronological techniques the samples were labeled, dried at room temperature, and then polished with progressively thinner sandpaper (60–1500 grain) to allow for the visualization of anatomical structures within the rings and thus the identification of the TRW boundaries (Stokes and Smiley, 1968). The tree-ring growth variations in each sample were visual crossdating under a binocular microscope (Stokes and Smiley, 1968) and measured to a precision of 0.001 mm using a Velmex system. The dating quality controlled was conducted using the program COFECHA (Holmes, 1983). The calendar dates to each tree ring were assigned following the Schulman convention for the Southern Hemisphere (Schulman, 1956) that uses the year when tree-ring formation starts (~November in our study site, Fig. 1b).

The ring-width measurements were standardized by fitting a negative exponential curve for each individual TRW series to remove variability not related to climate such as tree size-age trends (Cook and Kairiukstis, 1990). This detrending of the raw TRW measurements results in a set of dimensionless growth indices with a defined mean of 1.0. This allows the standardized indices from many samples to be averaged into a single TRW chronology. Finally, a residual chronology was obtained using the statistical package R "dplR" (Bunn, 2008) by averaging the individual standardized time series after the removal of the serial autocorrelation using an autoregressive modeling (Cook and Kairiukstis, 1990). The residual instead of standard chronology was selected for analyses as it emphasizes the high frequency variations of the climate signal contained in the TRW series and improves the climate-growth relationship (Gilman et al., 1963). The quality and sensitivity of the TRW chronology was assessed by the Mean Sensitivity (MS), the Expressed Population Signal (EPS), and the mean correlation between the TRW series (Rbar) (Wigley et al., 1984; Briffa, 1999). The MS represents a measure of the interannual variability in tree rings (Fritts, 1976), the Rbar the average of the correlation coefficients that result from comparing all possible pairs of segments of a given length among all TRW series that integrate a chronology (Briffa, 1999), and the EPS measures the strength of the common signal in the chronology by comparing a finite sample chronology with a hypothetical chronology that has been infinitely replicated (Wigley et al., 1984). While there is no level of significance for EPS, the value above 0.85 is generally accepted as a good level of common signal fidelity between trees (Wigley et al.,

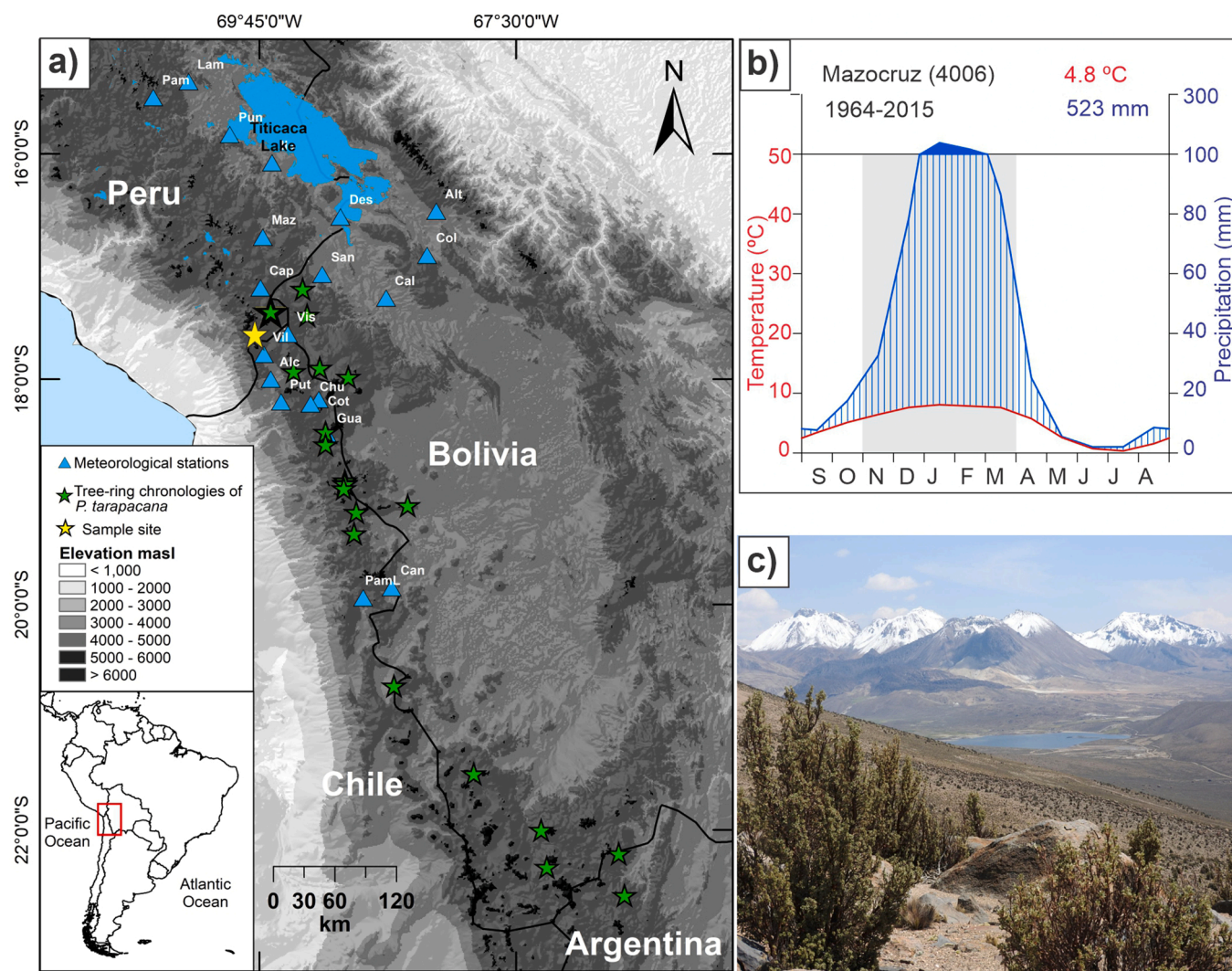


Fig. 1. Map of the study region in the South American Altiplano indicating the new *P. tarapacana* TRW site in Chiluyo (yellow star) and the present *P. tarapacana* TRW network (green stars, from Morales et al., 2020). The light blue triangles indicate the geographical location of the 20 meteorological stations in Peru, Bolivia and Chile, used in this study (a). Walter-Lieth climatic diagrams for the study site. Solid dark areas represent the wet season with monthly precipitation ≥ 100 mm. The humidity period (blue vertical lines) from November to March coincides with the spring-summer vegetation growing season (gray area) (b). Picture of our study site: *P. tarapacana* forest in the Peruvian Altiplano (c). (For interpretation of the references to color in this figure legend, the reader is referred to the web version of this article.)

1984). To calculate the running Rbar and EPS we used a 50-year window with an overlap of 25-year between adjacent windows.

All the chronologies from the *P. tarapacana* network were detrended using the same negative exponential standardization method used for the Chiluyo tree-ring chronology development. The residual chronologies were also computed by using autoregressive modeling to remove the serial autocorrelation in the original tree-ring series. The residual chronologies were used in the correlation analyses with the SSTs_N3.4 and the tree-ring chronology from Chiluyo. All the *P. tarapacana* chronologies shown in Fig. 1a were used for these analyses, except for the Huarikunka and Serke TRW chronologies that were discarded due to low replication and short time span (Supplementary material, Table S2).

2.3. Climate data

To assess the climate seasonality for the region monthly precipitation and temperature data were compiled from the meteorological national services from Chile (DMC), Peru and Bolivia (SENAMHI). We selected 20 meteorological stations located higher than 3500 m a.s.l. between 15°S and 20°S which presented less than 10% of missing data (Supplementary

material, Table S1). Linear regression models were used to fill missing data for an specific station using neighbor stations data (Ramos-Calzado et al., 2008). A correlation matrix computed for precipitation and temperature records from the selected meteorological stations show significant and positive correlations among data from different stations with a mean correlation coefficient of 0.66 among precipitation data (Fig. S1) and 0.56 among temperature data (Fig. S2). Based on this good agreement, regional indices of precipitation and temperature (1967–2015) were obtained averaging normalized data (z-score) from each station for the common periods when data was available (Jones and Hulme, 1996).

Finally, in order to assess the ENSO signal in the TRW chronologies, the Sea Surface Temperature anomalies from the Niño 3.4 region (SST_N3.4) for the period 1856–2015, were downloaded from the NOAA ERSSTv5 database (Huang et al., 2017).

2.4. Climate-growth relationships

Pearson's correlation analysis at 95% significance level were performed to assess the climate-growth relationships between the Chiluyo TRW chronology and precipitation/temperature (1967–2015) and

SST_N3.4 (1856–2015) data. Because tree radial growth could be influenced by climatic conditions from the previous growing year, the analyses were performed for 23-month period from June of two previous years to May of the current year (Blasing et al., 1984; Fritts, 1971). Based on the months with higher correlations with tree-growth), regional monthly indices of temperature (November–March from the current growing season), precipitation (November–January from the previous growing season) and SST_N3.4 (September–February from the current growing season) were computed.

Finally, we used boxplots to compare the values of the TRW chronology, precipitation and temperature during the years of El Niño (+ENSO = SST_N3.4 > 75th percentiles) and La Niña (-ENSO = SST_N3.4 < 25th percentiles). The Kolmogorov-Smirnov test was used to determine if there were significant differences ($p < 0.05$) in TRW, precipitation and temperature values between +ENSO and -ENSO - years.

2.5. Spectral properties for ENSO and *P. tarapacana* chronology

To identify periodicities and oscillatory modes in the time series, we performed a Continuous Wavelet Transform analysis -WT- (Torrence and Compo, 1998) for the Chiluyo TRW chronology and Niño 3.4 records during their common period. We also evaluated causal relationships in the time-frequency space between *P. tarapacana* growth from the Chiluyo site and ENSO variability (SST_N3.4) using the Cross Wavelet Transform analysis -XWT- (Grinsted et al., 2004). The XWT analysis finds regions in the time frequency space with high common spectral power and determine if both series are physically related (Jevrejeva et al., 2003). Monte Carlo methods were used to assess statistical significance against red noise backgrounds (Grinsted et al., 2004).

2.6. Spatial patterns of tree growth variations and ENSO sensitivity

To evaluate the spatial correlation pattern between the *P. tarapacana* TRW record from the Chiluyo site and the Pacific Ocean SST, we calculated field correlations (1856–2015) between the TRW chronology

and mean September–February gridded SST from the current growing season from the $2.5^\circ \times 2.5^\circ$ NCEP reanalysis global database (Kistler et al., 2001) using the KNMI Climate explorer tool (Trouet and Van Oldenborgh, 2013).

To compare the Chiluyo TRW record with the existent *P. tarapacana* TRW network across the Altiplano (Fig. 1a, Supplementary material Table S2), we performed correlation analysis between our record and each *P. tarapacana* chronology for their common period (1856–2001 CE). We also computed Pearson's correlations coefficients between all the *P. tarapacana* chronologies and the September–February SST_N3.4 records to assess ENSO sensitivity across the latitudinal gradient of the TRW network for the common period (1856–2001 CE). Additionally, to evaluate the intensity of these relationships between periods of high and low ENSO activity (Torrence and Webster, 1999) correlations among all the *P. tarapacana* TRW chronologies and correlations between each TRW chronology and September–February SST_N3.4 were computed for periods of high (1856–1930 CE, 1960–2001 CE) and low (1930–1960 CE) ENSO activity.

3. Results

3.1. The *Polylepis tarapacana* tree-ring chronology at Chiluyo

A total of 60 TRW series from 30 trees (i.e. 70% of the 43 tree samples collected) were used to develop a 414-year TRW chronology at a *P. tarapacana* forest close to the village of Chiluyo (Fig. 2a). This forest is located at the northwestern phytogeographical distribution of *P. tarapacana*.

The residual TRW chronology spans from 1602 to 2015 with more than 10 time series after 1666. The chronology has a MS of 0.29 that indicates high sensitivity (i.e. high year-to-year variability) and Rbar of 0.36 that indicates a common pattern in the interannual variations of radial growth among the individual series that composed the chronology. The mean EPS, which expresses the quality of a chronology, was 0.92 for the period from 1674 to 2015, which indicates that the number of trees used is suffice to represent the common growth pattern of this

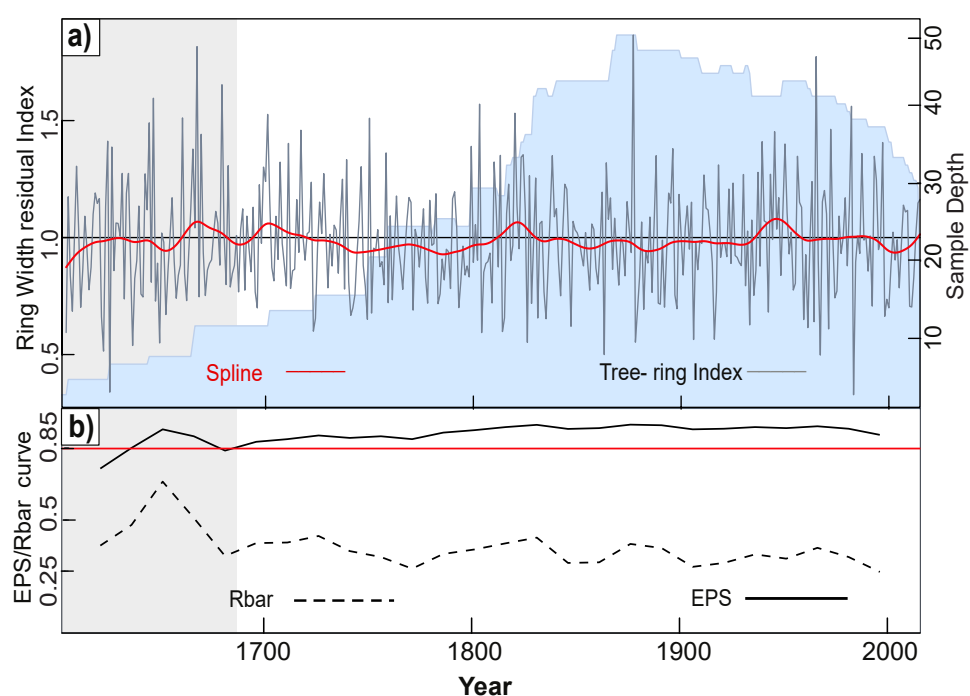


Fig. 2. (a) The residual TRW chronology of *P. tarapacana* (gray line), sample depth (light blue shaded area) and a 50-yr spline (red line). (b) The EPS and Rbar statistics were calculated using a 50-year moving window with an overlap of 25 years. The light gray shading area indicate the period 1602–1673 with low sample depth and EPS below 0.85. (For interpretation of the references to color in this figure legend, the reader is referred to the web version of this article.)

stand in Chiluyo.

3.2. Relationship between climate and radial growth

The Pearson's correlation coefficients between the residual TRW *P. tarapacana* chronology and precipitation/temperature data for the period 1967–2015 show contrasting responses of tree growth to climate between consecutive growth periods (Fig. 3a, b). A significant positive relationship ($P < 0.05$) was found between tree growth and the regional precipitation time series (Fig. 3a) for spring-summer months November to January (NDJ) of the previous growing season, while negative correlations were found during the current summer months from January to March (JFM). Tree growth exhibited positive correlations with monthly regional temperature from October to April (Fig. 3b) and monthly SST_N3.4 data from June to April (Fig. 3c) during the current growth season. Additionally, some discontinuous negative significant correlations ($P < 0.05$) were also reported during the previous growing season (Fig. 3b, c). Because of SST_N3.4 has high monthly auto-correlation, the correlation coefficients were significant for several months showing negative correlation with previous winter-spring and summer season (two previous June to previous September) and a shift to positive correlation from previous April to current May, albeit being significant

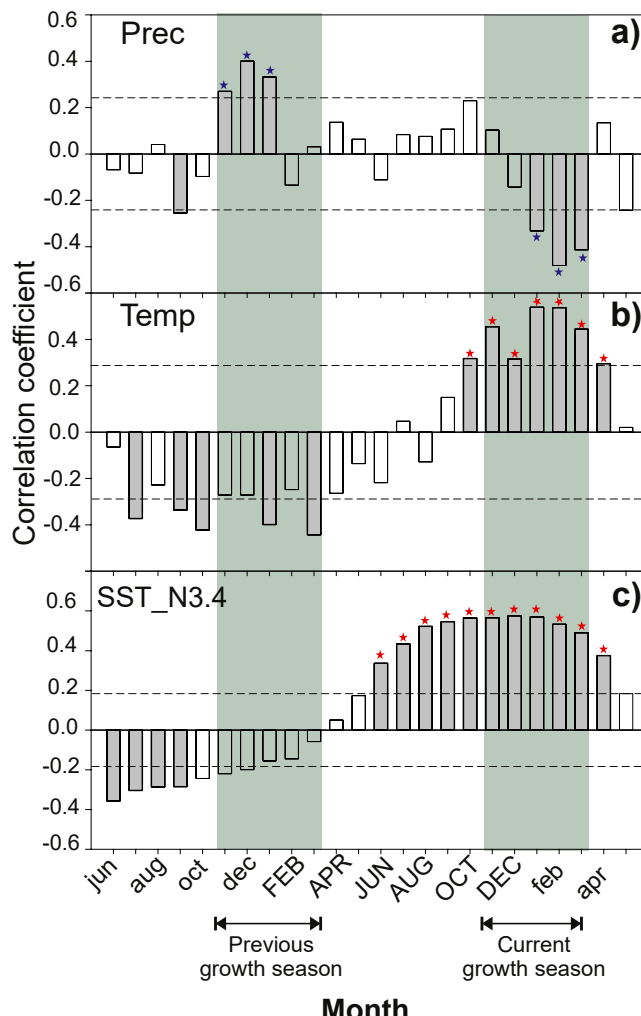


Fig. 3. Pearson's correlation coefficients between *P. tarapacana* residual ring-width chronology and monthly precipitation (a), temperature (b) and SST_N3.4 (c) from the two prior to the current year of ring formation. Dashed lines represent the 95% significant confidence levels. The green vertical shading indicate our suggested previous and current growing season for *P. tarapacana*.

from previous June to current April (Fig. 3c).

Tree growth variations of *P. tarapacana* are positive significantly correlated with regional NDJ precipitation from the previous season ($r = 0.52$, $P < 0.001$, Fig. S1a) and with regional temperature from November to March from the current growing season ($r = 0.59$, $P < 0.001$, Fig. S1b) for the period 1967–2015. Similarly, high correlations between tree growth and the SST_N3.4 from September to February are positive and significant for the period 1856–2015 ($r = 0.58$; $P < 0.001$, Fig. 4a).

Fig. 4 shows a good agreement between positive and negative extreme SST_N3.4 years with wide and narrow rings, respectively. We identified a total of 40 (41) years with values of SST_N3.4 above (below) the percentile 75th (25th) for the period 1856–2015. A 55% of these years (22 from 40) with positive SST_N3.4 anomalies (> 75 th percentile) representing El Niño conditions were coincident with wide rings years (Fig. 4a, b). A 44% of the years (18 from 41) with negative SST_N3.4 anomalies (< 25 th percentile) corresponding to La Niña conditions were concurrent with narrow rings years (Fig. 4a, b). We also found lower precipitation than average during El Niño years than during La Niña years (Fig. 4c) and higher temperatures than average during El Niño years than during La Niña years (Fig. 4d). Overall during El Niño (La Niña) years, the ring-width index (Fig. 4b) and temperature anomalies (Fig. 4d) were significantly above (below) the historical average, while precipitation anomalies were significantly below (above) the historical average (Fig. 4c). The difference between TRW, temperatures, and precipitation data during years of the ENSO + and ENSO- were significant ($P < 0.005$) based on the KS-Test.

We also identified that previous growing season extreme wet years (> 75 th percentile) coincide with high TRW, while extreme dry years (< 25 th percentile) are concurrent with low TRW values (Fig. S1a). The differences in the distribution of the TRW data between extreme wet and dry years were significant based on the KS-Test ($p < 0.005$, Fig. S1a). Likewise, during the current growing season extreme warm years (> 75 th percentile) coincide with high TRW values, while extreme cold years (< 25 th percentile) are concurrent with low TRW values (Fig. S2b). The distribution of TRW values during the warm and cold years is significantly different based on the KS-Test growth ($p < 0.005$, Fig. S1b). Overall these results suggest that previous season rainfall and current temperatures are key factors for tree growth with high (low) prior year precipitation and high (low) current temperatures favoring (constraining) wood formation.

3.3. Spatial pattern and spectral properties of the *P. tarapacana* TRW chronology and ENSO

Fig. 5a shows the spatial correlation patterns between the *P. tarapacana* TRW chronology and the global spatially explicit sea surface temperatures (SSTs) averaged for the current spring-summer season (September–February) for the period 1856–2015. Significantly positive correlations were found between the TRW record and Sep-Feb SST data over the equatorial Pacific Ocean region from 80 to 185°W longitude and 15°S to 15°N latitude. The significant correlation coefficients were higher in the El Niño 3.4 sector (~170°W to 120°W and 5°S to 5°N, $r > 0.5$), resembling a clear ENSO-like pattern.

The Wavelet spectrum analysis (WT) for the TRW record exhibits strong inter-annual and sub-decadal variability in a non-continuous way and significantly throughout the analyzed period from 1870 to 2015 (Fig. 5b). The periods with significant spectral power ($p < 0.05$) were detected at 2–6-year band around 1880 and 1960–1990, as well as in lower frequencies at 6–8 years band around 1900 and 1945–1965. Similarly, the WT for the SST_N3.4 time series shows significant spectral variability in the inter-annual frequency (2–6-year band) around 1880, 1900, 1980, 1990 and 2010, as well as significant power spectrum at 6–8-year band around 1910–1920 and 1940–1955 (Fig. 5c).

The cross-wave transformation (XWT) between the TRW chronology and the SST_N3.4 from September to February (spanning the period of

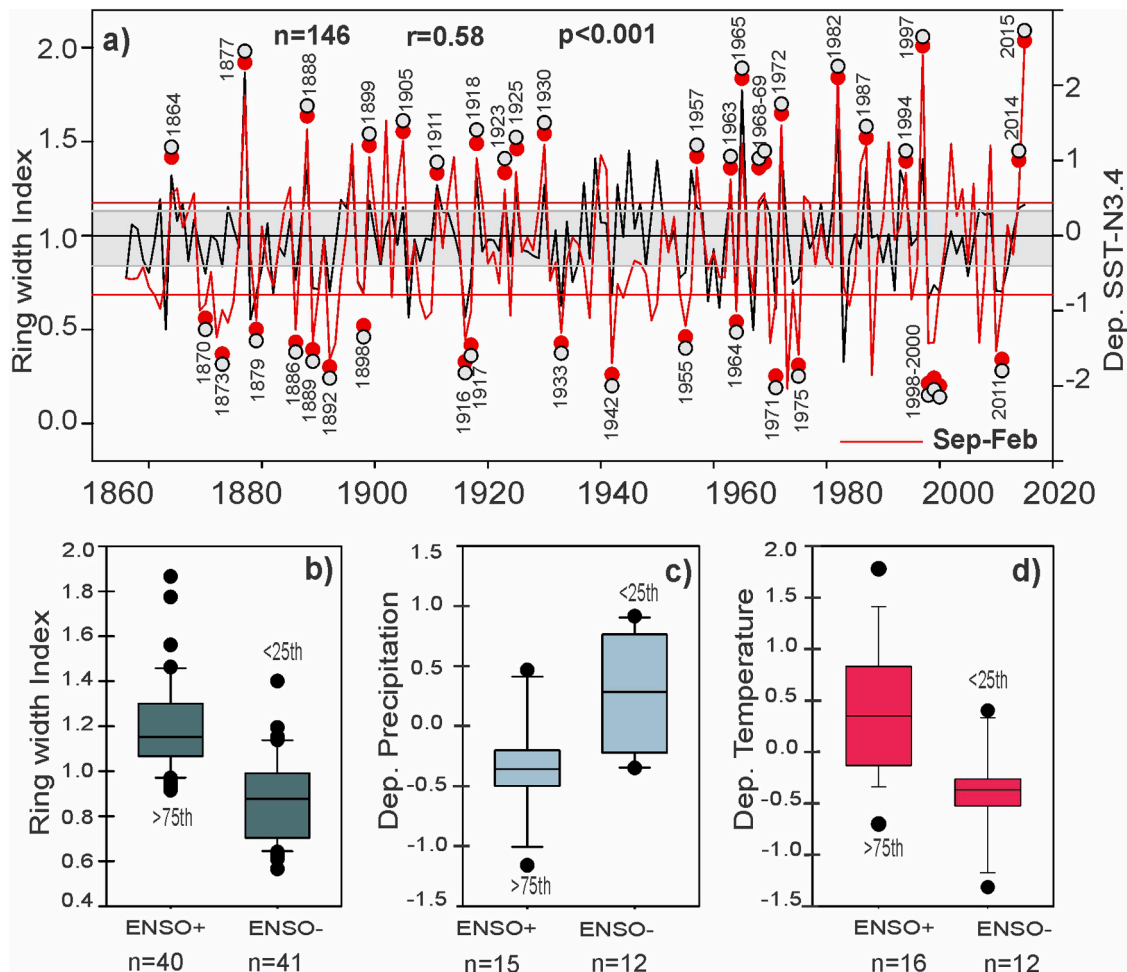


Fig. 4. (a) Comparison between the Chiluyo *P. tarapacana* TRW chronology and mean September-February SST_N3.4 for 1856–2015 period. The gray shading and the horizontal red lines indicates TRW indices and SST_N3.4 values within its 75th and 25th percentile distribution, respectively. The empty and red circles indicates extreme TRW and SST_N3.4 values, respectively. Box plots of the (b) *P. tarapacana* TRW for the period 1856–2015, and (c) precipitation and (d) temperature for the period 1967–2015 during the El Niño and La Niña years according to SST_N3.4 values > 75 th and < 25 th percentiles, respectively. (For interpretation of the references to color in this figure legend, the reader is referred to the web version of this article.)

highest ENSO activity) shows a common spectral power within the domain of 2–8-years (Fig. 5d) that corresponds to the width of the ENSO band (Fig. 5c). This XWT spectrum shows strong common signal of 2–4.5-year (1880–1890), 6–8.5 year (1900–1920), 6–7.5 year (1940–1960) and 2–4 year (1965–1975). Strong but short signals every 2–6 year also occurred between 1980 and 1983 and around 1998. However, there is a marked lack of common spectral power at 2–5 years cycles from 1900 to 1960 (XWT; Fig. 5c).

3.4. Tree-ring variability and ENSO sensitivity across the *P. tarapacana* network

The correlation coefficients between the Chiluyo *P. tarapacana* residual TRW chronology generated in this study and the 18 *P. tarapacana* residual TRW chronologies selected from an existing *P. tarapacana* network (Supplementary material, Table S2) are shown in Fig. 6a. All the correlation coefficients were significant and range between 0.41 and 0.78 (1856–2001). This indicates large similarities in TRW variations across the South American Altiplano. In general, our study site shows higher correlation coefficients with the geographically closer northern chronologies than with the southern chronologies, with the exception of some chronologies located in southwestern locations in the Argentinean Altiplano which also show high correlations coefficients with our site (Fig. 6a).

The correlation coefficients between the September-February SST_N3.4 and each *P. tarapacana* TRW chronologies of the network for the common period 1856–2001 show higher values for the northern chronologies ($r > 0.4$) than for the southern chronologies ($r < 0.23$). Among all the chronologies the newly TRW chronology from Chiluyo showed the highest correlation coefficient ($r = 0.48$) with the September-February SST_N3.4 (Fig. 6b). The decrease in correlation coefficients from north to south was not significant, in part because two southeastern TRW chronologies located in slightly wetter sites showed high correlation coefficients ($r = 0.46$) with SST_N3.4 with a similar strength than the northern TRW chronologies.

The same correlation analyses done for three periods of distinct ENSO intensity (high: 1856–1930 and 1960–2001; low: 1930–1960) show the same patterns (Fig. 6c, d). This indicates that the spatial patterns reported are consistent regardless of the non-stationary influence of ENSO on tree-growth variability of the *P. tarapacana* forests across the Altiplano. During the periods of high ENSO activity, the agreement (i.e. correlations) in tree growth variability between our site and the rest of the *P. tarapacana* chronologies was significant and higher than during the period of low ENSO activity (Fig. 6c). Similarly, correlation coefficients between September-February SST_N3.4 and *P. tarapacana* tree growth variability at each site were significant and higher during periods of high ENSO activity than during periods with low ENSO activity (Fig. 6d).

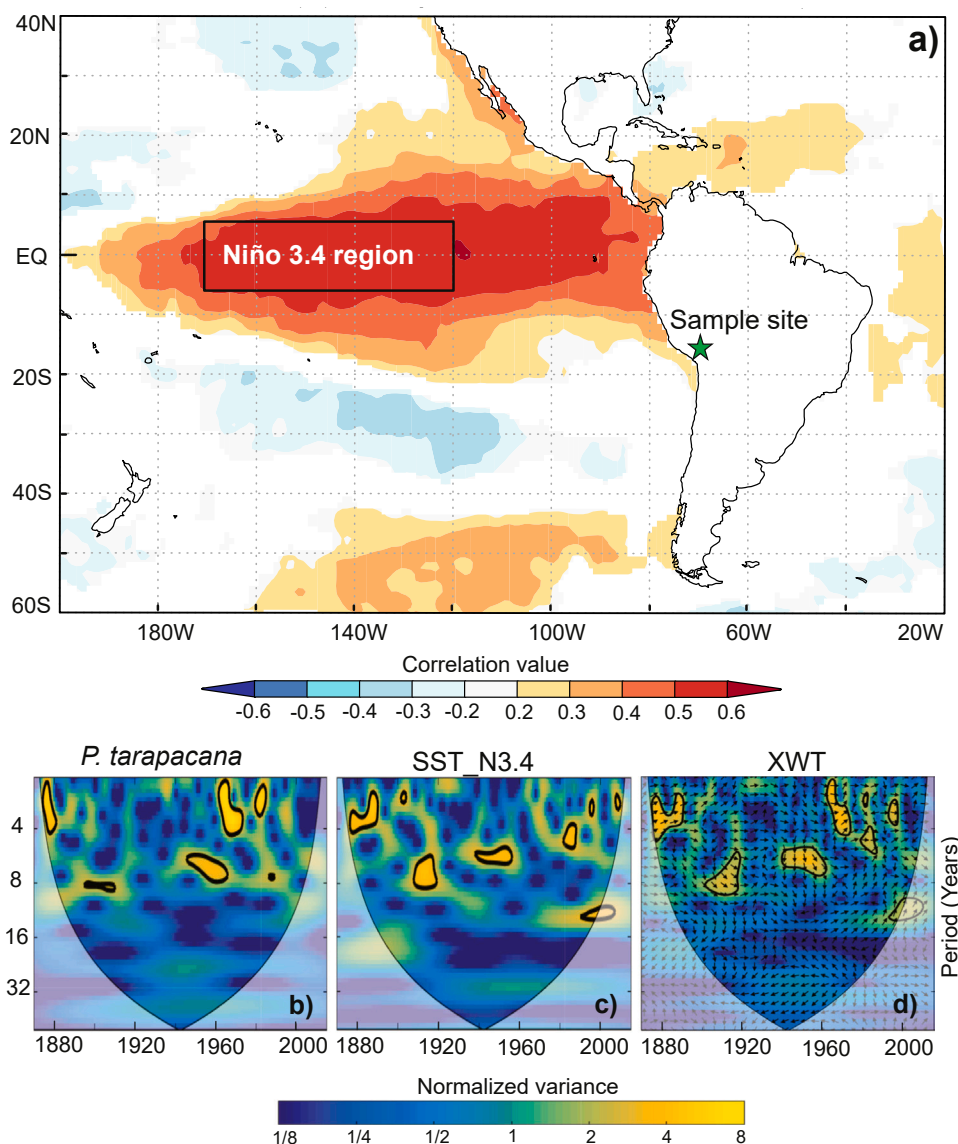


Fig. 5. (a) Spatial correlation between the *P. tarapacana* TRW chronology from Chiluyo (green star) and the $2.5^\circ \times 2.5^\circ$ gridded monthly averaged September-February Sea Surface Temperature (SST). The TRW chronology site is indicated by green star and colored fields represent significant ($p < 0.10$) Pearson correlation coefficients (a). Wavelet power spectrum (Morlet) of the TRW chronology (b) and the N3.4 SST record (c), and the cross wavelet transform (XWT) between the TRW chronology and N3.4 SST (September-February) (d). Black thick contours indicate the 95% level of significance using the red noise model, and the cone of influence is shown as a lighter shade. Vectors indicate the relative phase relationship between the TRW chronology and the SST_N3.4 (horizontal arrows pointing right and left implies in-phase and anti-phase relationships respectively, and pointing up means the second series lag the first by 90°). (For interpretation of the references to color in this figure legend, the reader is referred to the web version of this article.)

4. Discussion

4.1. *Polylepis tarapacana* radial growth variability across the Altiplano

In this study, we generated a centennial TRW chronology of *P. tarapacana* spanning from 1602 to 2015. This high replicated chronology represents the longest TRW record developed in Peru so far and extends northward the *P. tarapacana* TRW network to the limit of its geographical distribution. Although there is another TRW chronology of this species located further north (17.2°S) at Cerro Huarinka in Bolivia (Fig. 1a; see Solíz et al., 2009), its use for dendroclimatological studies have been limited due to a short time span of less than 100 years (1925–1999) and low sample replication ($N < 10$ time series). Our newly developed TRW chronology has high-quality statistics with similar values than reported in previous published chronologies from the South American Altiplano (Argollo et al., 2004; Christie et al., 2009; Solíz et al., 2009).

The growth variability of our TRW record is highly correlated with the 18 *P. tarapacana* TRW chronologies distributed across the Altiplano, with the highest correlations found with the nearby chronologies to our study site (northern Altiplano; Fig. 6a, c). This agreement in tree growth variability among *P. tarapacana* forests over the Altiplano reflects the

influence of large macroclimatic signals on tree growth variations and it is consistent with a previous study from Solíz et al. (2009). However, the significant decrease in the correlations following the north-south latitudinal gradient reports differences of growth variability between the northern and southern chronologies, which could be related to distinct influence of local and regional climate on tree growth across the Altiplano.

4.2. Tree-growth climate sensitivity from a northern *Polylepis tarapacana* population

P. tarapacana trees located in the South American Altiplano are exposed to long period of aridity and frequent frost events any time throughout the year (García-plazaola et al., 2015; Hoch and Körner, 2005). *P. tarapacana* growth in such harsh environment tends to be limited mainly by water deficits (Morales et al., 2004) and low temperatures (Hoch and Körner, 2005). Our results confirm that *P. tarapacana* growth variability at the northern region of the Altiplano is strongly related with local and regional precipitation and temperature. These findings are consistent with previous studies developed at the Chilean, Bolivian and Argentinean Altiplano that showed a positively (negatively) influenced by previous (current) spring-summer

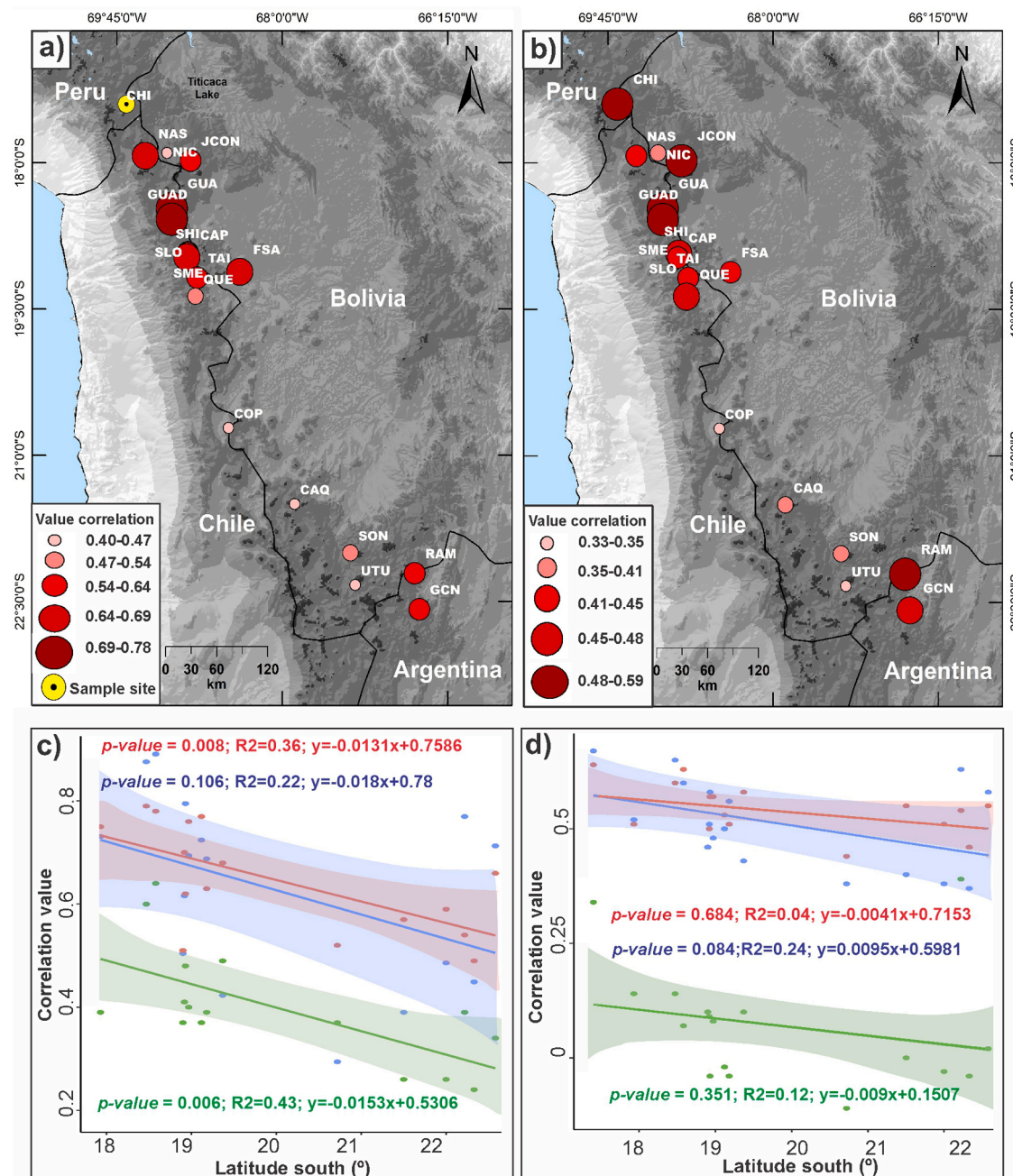


Fig. 6. (a) Correlation map between the northernmost *P. tarapacana* chronology represented by the Chiluyo site (yellow dot) and the available *P. tarapacana* network during the common period 1856–2001. (b) Correlation map between all *P. tarapacana* chronologies and SST_N3.4 for the 1856–2001 period. (c) Scatter plot of the correlations results from (a) and (b) vs. latitude for three periods of ENSO activity: red 1856–1930, green 1930–1960 and blue 1960–2001 (c and d, respectively). (For interpretation of the references to color in this figure legend, the reader is referred to the web version of this article.)

season precipitation and positive (negative) influence by current (previous) spring-summer temperatures on *P. tarapacana* radial growth (Argollo et al., 2004; Morales et al., 2004; Moya and Lara, 2011; Rodriguez-Catón et al., 2021; Solíz et al., 2009).

The opposite climate response pattern of *P. tarapacana* growth between the two consecutive growth seasons is consistent throughout its latitudinal distribution range (Rodríguez-Catón et al., 2021). In the Altiplano, temperature and precipitation are associated through a negative relationship that is more strong during the rainy season (Ramos-Calzado et al., 2008; Rodriguez-Catón et al., 2021). The lack of independence between both variables can mask the individual effects of each climate variable on tree growth. In other words, a negative response of tree growth to rainfall during the current growth period may not imply

that water is detrimental to growth since it could be associated to more cloudiness and lower temperatures that may be indeed the limiting factors for growth.

Water availability of the previous growing season is critical for tree growth all along the Altiplano, but especially in the arid south (Argollo et al., 2004; Morales et al., 2004). An ecophysiological study ~180 km south of our study site in the Chilean Altiplano reported that in this tree species (1) photosynthetic processing and carbon assimilation are well adapted to cope with low temperatures, (2) photosynthesis and carbon assimilation occur mainly during the morning taking advantage of low vapor pressure deficit (VPD). Low VPD allows for larger stomatal aperture than during midday and afternoon when photosynthetic activity is limited by stomatal closure due to high VPD (García-Plazaola

et al., 2015). These results pointed out the increase in VPD as a key limiting factor in carbon assimilation for *P. tarapacana*, especially towards the south of its distribution.

Temperature seems to favor tree growth in the wetter northern Altiplano during the current growing season (Fig. 3b). In agreement, Rodriguez-Caton et al. (2021) reported that water availability in the northern Altiplano may not be as limiting as in the arid southern Altiplano, and thus warmer conditions during the growing season may favor both TRW formation and carbon assimilation. Based on TRW and stable isotopes ($\delta^{13}\text{C}$ and $\delta^{18}\text{O}$) data from four *P. tarapacana* populations along a 500 km latitudinal gradient ($\sim 18^\circ\text{S}$ - 22°S). Rodriguez-Caton et al. (2021) also reported that *P. tarapacana* growth was mainly influenced by temperature in northern wetter sites and by water availability in the southern drier regions of the Altiplano, which is also consistent with our results and illustrates the complexity of the climatic variable controlling tree growth in these forests. Rodriguez-Caton et al. (2021) also pointed out that there are differences in growth response to these variables that are related to the north-south aridity gradient along the Altiplano and suggests that the relative importance of temperature and precipitation in regulating tree growth depends largely on local water availability, but in any case, both variables are involved in growth ring formation. In summary, we can conclude that optimal growth condition for *P. tarapacana* forests in the northern Altiplano occur with wet spring-summer in the previous season and warm conditions during the spring-summer of the current growing season.

4.3. The ENSO imprint in the *Polylepis tarapacana* TRW chronologies

We found the strongest ENSO signature in the Chiluyo *P. tarapacana* TRW chronology generated for this study from 1856–2015 ($r = 0.58$) as well as for the common period for the tree-ring network ($r = 0.48$, 1856–2001). The strong relationship between this TRW record and the September–February SST_N3.4 anomalies indicates that the atmospheric circulation modulated by the tropical Pacific in a positive ENSO phase may lead to local climatic conditions that will positively influence *P. tarapacana* growth. This reflects well the large-scale ENSO influence on climate from Peruvian Altiplano associated to warm temperatures and low precipitation (Fig. 4c, d; Garreaud et al., 2009; Garreaud and Aceituno, 2001; Lagos et al., 2008; Lavado-Casimiro and Espinoza, 2014; Vuille et al., 2000).

The ENSO signal on the TRW chronologies was also analyzed across the entire Altiplano and we observed high correlation coefficients between ENSO and the northern TRW chronologies ($r > 0.4$). However, some TRW chronologies located in the southeast of the tree-ring network achieved similar correlation coefficient values ($r > 0.4$). Remarkably, the lowest correlation values between the September–February SST_N3.4 and the *P. tarapacana* TRW chronologies were located at the southwestern area, which is the driest sector of this tree-ring network with a strong influence of the Atacama Desert (Fig. 8 in Rodriguez-Caton et al., 2021). There is a differential ENSO imprint across the Altiplano regarding general positive (negative) temperature and negative (positive) precipitation anomalies during El Niño (La Niña) events (Vuille 1999; Garreaud et al. 2009), which can be associated to the distinct ENSO sensitivity recorded across the network. Our interpretation is that the warmer and drier conditions resulting by the El Niño events may favor radial growth of trees located in humid environments at the northern and southeastern sites, while trees growing in more arid southwestern locations may not be benefited by this warmer and drier extreme conditions associated to positive ENSO during the current year of growth. We concluded that the local aridity conditions are an important factor determining the strength of the ENSO signal across the *P. tarapacana* TRW chronologies.

P. tarapacana TRW and the SST_N3.4 data shows similar oscillations modes mainly from 2 to 8-year bandwidth indicating consistencies between both time series. These oscillatory modes found at our study site at the Peruvian Altiplano are consistent with the spectral properties

previously recorded in two *P. tarapacana* populations from the southern portion of the Altiplano (Christie et al., 2009). This common spectral power is not continuous throughout time probably associated to the non-stationarity behavior of ENSO (Torrence and Webster, 1999). The lack of stationarity between ENSO and *P. tarapacana* growths at high frequency variability was previously reported by Morales et al. (2012).

We also found that the growth synchronicity among our study site and the rest of *P. tarapacana* forest along the Altiplano, as well as the relationships between tree growth at all sites and the SST_N3.4 was stronger during periods of high ENSO activity of during low ENSO activity. This may indicate a possible loss of a high frequency macro-climatic signal related to ENSO. These results confirm that *P. tarapacana* TRW records are extremely useful to develop ENSO reconstructions utilizing large TRW networks, being capable to significantly increase the accuracy of this kind of reconstructions that have mostly depended on extratropical proxy records (Li et al., 2013).

5. Conclusions

A 414-year TRW width chronology of *P. tarapacana* spanning from 1602 to 2015 was generated in the Peruvian Altiplano. This paleo record represents the longest TRW chronology developed in Peru. Our findings show that *P. tarapacana* growth in its northern distribution is favored by warm, but not very wet conditions during the season of tree-ring formation, but by wet conditions during the previous growing season to the tree-ring formation. The presence of the ENSO signal recorded by the TRW data provides, evidence of the strong influence of tropical Pacific temperatures on *P. tarapacana* growth. The highest spatial correlation between the TRW chronology with the tropical Pacific SST from sector 3.4 shows the high reconstruction skill of *P. tarapacana* as reliable proxy of past ENSO variability. This new paleo record is of great scientific relevance for future climate and ENSO reconstructions, offering an additional tropical TRW record from a region where the interannual climatic variability is strongly modulated by the behavior of this large-scale climate forcing. Moreover, our new record expands and strengthens the present network of tropical TRW chronologies in South America which is still in its infancy compared to mid and high latitudes, highlighting the need for further tree-ring research in this region.

Funding

This study was supported by Proyecto CONCYTEC – Banco Mundial (FONDECYT-BM-INC. INV 039-2019), Peru. M.S.M. was supported by Agencia Nacional de Promoción Científica y Tecnológica (ANPCyT), (PICT 2013-1880) and CONICET (PIP 11220130100584), Argentina. L. A.-H. and M.S.M. were supported by the US National Science Foundation (NSF) AGS-1702789, AGS-1903687 and OISE-1743738, USA, and by The THEMES project funded by the BNP Paribas Foundation in the frame of its 'Climate Initiative' program. D.A.C. was supported by FONDECYT 1201411 and ANID/FONDAP/15110009, Chile.

Declaration of Competing Interest

The authors declare that they have no known competing financial interests or personal relationships that could have appeared to influence the work reported in this paper.

Acknowledgments

Doris dedicates this article for her first baby. Also, she is grateful to: Ginette Ticse, Osir Vidal, Harold Quispe (for the support with the maps), Vladimir Camel, Fressia Ames, Ernesto Chanes for their suggestions that greatly improved this work.

CRediT authorship contribution statement

E.J.R.R. and M.S.M conceived the study, collected field samples and supervised chronology development. D.B.C. generated the TRW chronology and write a first version of the manuscript. D.B.C. and E.J.R.R. conduct the data analyses with inputs from M.S.M and L.A.H. A.G prepared some samples and support with graphics. D.B.C, E.J.R.R., M.S.M and L.A.H elaborated the content manuscript. D.B.C wrote the first version of the manuscript and the E.J.R.R., D.A.C., M.S.M and L.A.H contributed substantially to manuscript revisions. All the authors read and provide inputs to the manuscript.

Appendix A. Supplementary material

Supplementary data associated with this article can be found in the online version at [doi:10.1016/j.dendro.2021.125902](https://doi.org/10.1016/j.dendro.2021.125902).

References

Andrade, M.F., 2018. Clima y eventos extremos del Altiplano Central perú-boliviano. *Geographica Bernensis*. (<https://doi.org/10.4480/GB2018.N01>).

A dendrochronology program library in R (dplR). *Dendrochronologia* 26, 2008, 115–124. (<https://doi.org/10.1016/j.dendro.2008.01.002>).

Argollo, J., Soliz, C., Villalba, R., 2004. Potencialidad dendrocronológica de *Polylepis tarapacana* en los Andes Centrales de Bolivia. *Ecol. Boliv.* 39, 5–24.

Blasing, T.J., Solomon, A.M., Duvick, D.N., 1984. Response functions revisited. *Tree-Ring Bull.* 44, 1–15.

Briffa, K.R., 1999. Interpreting high-resolution proxy climate data — the example of dendroclimatology. *Anal. Clim. Var.* 0500, 77–94. (https://doi.org/10.1007/978-3-662-03744-7_5).

Cavledes, C.N., 1985. Emergency and institutional crisis in Peru during El Niño 1982–1983. *Disasters* 9, 70–74. (<https://doi.org/10.1111/j.1467-7717.1985.tb00913.x>).

Christie, D.A., Lara, A., Barichivich, J., Villalba, R., Morales, M.S., Cuq, E., 2009. El Niño–Southern Oscillation signal in the world's highest-elevation tree-ring chronologies from the Altiplano, Central Andes. *Palaeogeogr. Palaeoclimatol. Palaeoecol.* 281, 309–319. (<https://doi.org/10.1016/j.palaeo.2007.11.013>).

Cook, E.R., Kairiukstis, L.A., 1990. *Methods of Dendrochronology: Applications in the Environmental Sciences*. Kluwer Academic, Dordrecht, The Netherlands.

Drenkhan, F., Carey, M., Huggel, C., Seidel, J., Oré, M.T., 2015. The changing water cycle: climatic and socioeconomic drivers of water-related changes in the Andes of Peru. *Wiley Interdiscip. Rev. Water* 2, 715–733. (<https://doi.org/10.1002/wat2.1105>).

Fritts, H.C., 1971. Dendroclimatology and dendroecology. *Quat. Res.* 1, 419–449. ([https://doi.org/10.1016/0033-5894\(71\)90057-3](https://doi.org/10.1016/0033-5894(71)90057-3)).

García-plazaola, J.I., Rojas, R., Christie, D.A., Rafael, E., 2015. Photosynthetic responses of trees in high-elevation forests: comparing evergreen species along an elevation gradient in the Central Andes. *AoB plants* plv058, pp. 1–40. (<https://doi.org/10.1093/aobpla/plv058>).

Fritts, Harold, 1976. *Tree rings and climate*. United States. Academic Press, New York.

Garreaud, R.D., 1999. Multiscale analysis of the summertime precipitation over the central Andes. *Mon. Weather Rev.* 127, 901–921. ([https://doi.org/10.1175/1520-0493\(1999\)127<0901:MAOTSP>2.0.CO;2](https://doi.org/10.1175/1520-0493(1999)127<0901:MAOTSP>2.0.CO;2)).

Garreaud, R.D., Aceituno, P., 2001. Interannual rainfall variability over the South American Altiplano. *J. Clim.* 14, 2779–2789. ([https://doi.org/10.1175/1520-0442\(2001\)014<2779:IRVOTS>2.0.CO;2](https://doi.org/10.1175/1520-0442(2001)014<2779:IRVOTS>2.0.CO;2)).

Garreaud, R.D., Vuille, M., Compagnucci, R., Marengo, J., 2009. Present-day South American climate. *Palaeogeogr. Palaeoclimatol. Palaeoecol.* 281, 180–195. (<https://doi.org/10.1016/j.palaeo.2009.10.032>).

Gilles, J.L., Valdivia, C., 2009. Local forecast communication in the altiplano. *Bull. Am. Meteorol. Soc.* 90, 85–91. (<https://doi.org/10.1175/2008BAMS2183.1>).

Gilman, D.L., Fuglister, F.J., Mitchell Jr., J.M., 1963. On the power spectrum of "red noise". *J. Atmos. Sci.* ([https://doi.org/10.1175/15200469\(1963\)020<0000:OEPSO](https://doi.org/10.1175/15200469(1963)020<0000:OEPSO)).

Grinsted, A., Moore, J.C., Jevrejeva, S., 2004. Application of the cross wavelet transform and wavelet coherence to geophysical time series. *Nonlinear Process. Geophys.* 11, 561–566. (<https://doi.org/10.5194/npg-11-561-2004>).

Hoch, G., Körner, C., 2005. Growth, demography and carbon relations of *Polylepis* trees at the world's highest treeline. *Funct. Ecol.* 19, 941–951. (<https://doi.org/10.1111/j.1365-2435.2005.01040.x>).

Holmes, R.L., 1983. Computer-assisted quality control in tree-ring dating and measurement. *Tree-Ring Bull.* 43, 69–78.

Huang, B., Thorne, P.W., Banzon, V.F., Boyer, T., Chepurin, G., Lawrimore, J.H., Menne, M.J., Smith, T.M., Vose, R.S., Zhang, H.M., 2017. Extended reconstructed Sea surface temperature, Version 5 (ERSSTv5): upgrades, validations, and intercomparisons. *J. Clim.* 30, 8179–8205. (<https://doi.org/10.1175/JCLI-D-16-0836.1>).

Jevrejeva, S., Moore, J.C., Grinsted, A., 2003. Influence of the Arctic oscillation and El Niño–Southern Oscillation (ENSO) on ice conditions in the Baltic Sea: the wavelet approach. *J. Geophys. Res. D Atmos.* 108, 1–11. (<https://doi.org/10.1029/2003jd003417>).

Jones, P.D., Hulme, M., 1996. Calculating regional climatic time series for temperature and precipitation: methods and illustrations. *Int. J. Climatol.* 16, 361–377. ([https://doi.org/10.1002/\(SICI\)1097-0088\(199604\)16:4<361::AID-JOC53>3.0.CO;2-F](https://doi.org/10.1002/(SICI)1097-0088(199604)16:4<361::AID-JOC53>3.0.CO;2-F)).

Josse, C., Cuesta, F., Navarro, G., Barrena, V., Cabrera, E., Chacón-Moreno, E., Ferreira, W., Peralvo, M., Saito, J., Tovar, A., 2009. Ecosistemas de los Andes del Norte y Centro. Bolivia, Colombia, Ecuador, Perú y Venezuela.

Kessler, M., Schmidt-Lebuhn, A., 2006. *Taxonomía y distribución de Polylepis. Org. Divers. Evol.* 6, 1–10.

Kistler, R., Kalnay, E., Collins, W., Saha, S., White, G., Woollen, J., Chelliah, M., Ebisuzaki, W., Kanamitsu, M., Kousky, V., Van Den Dool, H., Jenne, R., Fiorino, M., 2001. The NCEP–NCAR 50-year analysis: Monthly means CD-ROM and documentation. *Bull. Am. Meteorol. Soc.* 82, 247–267. ([https://doi.org/10.1175/1520-0477\(2001\)082<0247:TNNYRM>2.3.CO;2](https://doi.org/10.1175/1520-0477(2001)082<0247:TNNYRM>2.3.CO;2)).

Lagos, P., Silva, Y., Nickl, E., Mosquera, K., Lagos, P., Silva, Y., Nickl, E., Ni, K.M.E.L., 2008. El Niño-related precipitation variability in Perú. *Adv. Geosci.* 14, 231–237. (<https://doi.org/10.5194/adgeo-14-231-2008>).

Lavado-Casimiro, W., Espinoza, J.C., 2014. Impactos de el niño y la niña en las lluvias del Perú (1965–2007). *Rev. Bras. Meteorol.* 29, 171–182. (<https://doi.org/10.1590/S0102-7782014000200003>).

Li, J., Xie, S.P., Cook, E.R., Morales, M.S., Christie, D.A., Johnson, N.C., Chen, F., D'Arrigo, R., Fowler, A.M., Gou, X., Fang, K., 2013. El Niño modulations over the past seven centuries. *Nat. Clim. Chang.* 3, 822–826. (<https://doi.org/10.1038/nclimate1936>).

Morales, M.S., Carilla, J., Grau, H.R., Villalba, R., 2015. Multi-century lake area changes in the Andean high-elevation ecosystems of the Southern Altiplano. *Clim. Past Discuss.* 11, 1821–1855. (<https://doi.org/10.5194/cpd-11-1821-2015>).

Morales, M.S., Christie, D.A., Neukom, Raphael, Rojas, Facundo, Villalba, R., et al., 2018. *Variabilidad hidroclimática en el sur del Altiplano: pasado, presente y futuro. La Puna argentina: Naturaleza y cultura*, 1a. Fundación Miguel Lillo, pp. 75–91.

Morales, M.S., Christie, D.A., Villalba, R., Argollo, J., Pacajes, J., Silva, J.S., Alvarez, C., A., Llancabure, J.C., Gamboa, C.C.S., 2012. Precipitation changes in the South American Altiplano since 1300 AD reconstructed by tree-rings. *Clim. Past* 8, 653–666. (<https://doi.org/10.5194/cp-8-653-2012>).

Morales, M.S., Cook, E.R., Barichivich, J., Christie, D.A., Villalba, R., LeQuesne, C., Sru, A.M., Eugenia Ferrero, M., González-Reyes, Á., Couvreux, F., Matskovsky, V., Aravena, J.C., Lara, A., Mundo, I.A., Rojas, F., Prieto, M.R., Smerdon, J.E., Bianchi, L.O., Masiokas, M.H., Urrutia-Jalabert, R., Rodriguez-Catón, M., Muñoz, A., A., Rojas-Badilla, M., Alvarez, C., Lopez, L., Luckman, B.H., Lister, D., Harris, I., Jones, P.D., Park Williams, A., Velazquez, G., Aliste, D., Aguilera-Betti, I., Marcotti, E., Flores, F., Muñoz, T., Cuq, E., Boninsegna, J.A., 2020. Six hundred years of South American tree rings reveal an increase in severe hydroclimatic events since mid-20th century. *Proc. Natl. Acad. Sci. USA* 117, 16816–16823. (<https://doi.org/10.1073/pnas.2002411117>).

Morales, S., Villalba, R., Grau, R., Paolini, L., 2004. Rainfall-controlled tree growth in high-elevation subtropical treelines. *Ecology* 85, 3080–3089. (<https://doi.org/10.1890/04-0139>).

Moya, J., Lara, A., 2011. Tree rings chronologies of quenoa (*Polylepis tarapacana*) for the last 500 years in the Altiplano of Arica and Parinacota Region, Chile. *Bosque* 32, 165–173. (<https://doi.org/10.4067/S0717-92002011000200007>).

Neukom, R., Rohrer, M., Calanca, P., Salzmann, N., Huggel, C., Acuña, D., Christie, D.A., Morales, M.S., 2015. Facing unprecedented drying of the Central Andes? Precipitation variability over the period AD 1000–2100. *Environ. Res. Lett.* 10. (<https://doi.org/10.1088/1748-9326/10/8/084017>).

Ramos-Calzado, P., Gómez-Camacho, J., Pérez-Bernal, F.P.-L.M., 2008. A novel approach to precipitation series completion in climatological datasets: application to Andalusia. *Int. J. Climatol.* 29, 2011–2029. (<https://doi.org/10.1002/joc.2029>).

Rodríguez-Catón, M., Andreu-Hayles, L., Morales, M.S., Daux, V., Christie, D.A., Coopman, R.E., Alvarez, C., Rao, M.P., Aliste, D., Flores, F., Villalba, R., 2021. Different climate sensitivity for radial growth, but uniform for tree-ring stable isotopes along an aridity gradient in *Polylepis tarapacana*, the world's highest elevation tree-species. *Tree Physiol.* 41, 1353–1371. (<https://doi.org/10.1093/treephys/pab021>).

Schulman, E., 1956. *Dendroclimatic Changes in Semiarid América*. University of Arizona Press, Tucson.

Sietz, Diana, Mamani-Choque, Sabino, Ludeke, Matthias, et al., 2012. Typical patterns of smallholder vulnerability to weather extremes with regard to food security in the Peruvian Altiplano. *Regional Environmental Change* 12, 489–505. (<https://doi.org/10.1007/s10113-011-0246-5>).

Solíz, C., Villalba, R., Argollo, J., Morales, M., Christie, D., Moya, J., Pacajes, J., 2009. Spatio-temporal variations in *Polylepis tarapacana* radial growth across the Bolivian Altiplano during the 20th century. *Palaeogeogr. Palaeoclimatol. Palaeoecol.* 281, 296–308. (<https://doi.org/10.1016/j.palaeo.2008.07.025>).

Stokes, M.A., Smiley, T., 1968b. An Introduction to Tree-Ring Dating, Univ. Chic. ed.

Torrence, C., Compo, G., 1998. A practical guide to wavelet analysis. *Bulletin of the American Meteorological society* 79, 61–78. ([https://doi.org/10.1175/1520-0477\(1998\)079<0061:APGTWA>2.0.CO;2](https://doi.org/10.1175/1520-0477(1998)079<0061:APGTWA>2.0.CO;2)).

Torrence, C., Webster, P.J., 1999. Interdecadal changes in the ENSO-monsoon system. *J. Clim.* 12, 2679–2690. ([https://doi.org/10.1175/1520-0442\(1999\)012<2679:ICITEM>2.0.CO;2](https://doi.org/10.1175/1520-0442(1999)012<2679:ICITEM>2.0.CO;2)).

Trenberth, K.E., Caron, J.M., 2000. The southern oscillation revisited: Sea level pressures, surface temperatures, and precipitation. *J. Clim.* 13, 4358–4365. ([https://doi.org/10.1175/1520-0442\(2000\)013<4358:TSOSRL>2.0.CO;2](https://doi.org/10.1175/1520-0442(2000)013<4358:TSOSRL>2.0.CO;2)).

Trouet, V., Van Oldenborgh, G.J., 2013. KNMI climate explorer: a web-based research tool for high-resolution paleoclimatology. *Tree-Ring Res.* 69, 3–13. (<https://doi.org/10.3959/1536-1098-69.1.3>).

Vargas, P., 2009. El cambio climático y sus efectos en la salud. Banco Cent. Reserv. del Perú.

Vera, C., Báez, J., Douglas, M., Emmanuel, C.B., Marengo, J., Meitin, J., Nicolini, M., Nogués-Paegle, J., Paegle, J., Penalba, O., Salio, P., Saulo, A., Dias, M., Silva Dias, P., Zipser, E., 2006. The South American low-level jet experiment. Bull. Am. Meteorol. Soc. 87, 63–78. <https://doi.org/10.1175/BAMS-87-1-63>.

Vuille, M., 1999. Atmospheric circulation over the Bolivian Altiplano during dry and wet periods and extreme phases of the southern oscillation. Int. J. Climatol. 19, 1579–1600. [https://doi.org/10.1002/\(SICI\)10970088\(19991130\)19:14<1579::AID-JOC441>3.0.CO;2-N](https://doi.org/10.1002/(SICI)10970088(19991130)19:14<1579::AID-JOC441>3.0.CO;2-N).

Vuille, M., Bradley, R.S., Keimig, F., 2000. Climate variability in the Andes of Ecuador and its relation to tropical Pacific and Atlantic Sea Surface temperature anomalies. J. Clim. 13, 2520–2535. [https://doi.org/10.1175/15200442\(2000\)013<2520:CVITAO>2.0.CO;2](https://doi.org/10.1175/15200442(2000)013<2520:CVITAO>2.0.CO;2).

Wigley, T.M.L., Briffa, K.R., Jones, P.D., 1984. On the average value of correlated time series with applications in dendroclimatology and hydrometeorology. J. Clim. Appl. Meteorol. 23, 201–213. [https://doi.org/10.1175/15200450\(1984\)023<0201:OTAVOC>2.0.CO;2](https://doi.org/10.1175/15200450(1984)023<0201:OTAVOC>2.0.CO;2).